EPJ Web of Conferences **17**, 03002 (2011)
DOI: 10.1051/epjconf/20111703002

A complete picture of the breakup in ^{6,7}Li-induced reactions

D. H. Luong[1,a], D. J. Hinde[1], M. Dasgupta[1], M. Evers[1], R. Rafiei[1], and R. du Rietz[1]

Department of Nuclear Physics, Research School of Physics and Engineering, Australian National University, Canberra, Australian Capital Territory 0200, Australia

Abstract. Experiments with weakly-bound nuclei have demonstrated that breakup significantly affects the reaction outcomes. Coincidence measurements of breakup fragments at sub-barrier energies, using a position sensitive back-angle detector array covering 117° to 167°, have enabled the complete characterisation of the breakup processes in the reactions of the weakly-bound ^{6,7}Li with ^{208}Pb. The timescales of different breakup processes were also extracted from the fragments kinematics, enabling a clear characterization of prompt and delayed breakup. The majority of these prompt breakup events are triggered by *n*-stripping for ^{6}Li, and *p*-pickup for ^{7}Li. The demonstration that the reaction dynamics and outcomes can be significantly determined not only by the properties of the two colliding nuclei, but by the ground-state and excited state properties of their neighbours, is a key insight for understanding and predicting reactions of weakly-bound nuclei near the limits of nuclear existence.

1 Introduction

Dissociation of the weakly-bound ^{6}Li$\rightarrow \alpha + d$ and ^{7}Li$\rightarrow \alpha + t$ were observed experimentally in the early 70s [1–7]. Two different breakup modes were identified. The first being *direct* (non-resonant) breakup [8] where differential nuclear forces between the target and the projectile fragments [5,9] were believed to be the dominant contributor. The second breakup mode was *sequential* (resonant) breakup [10,11] which proceeds sequentially by first exciting the nuclei, via Coulomb excitation, to it continuum state which then dissociates into its cluster fragments. Further observations showed breakup triggered by nucleon transfer [12–14] also played an important role. More recent observations of suppression of complete fusion ($\sim$ 30%) in reactions of Li was generally associated with their low breakup threshold energies [15–17]. Measurements of sub-barrier breakup fragments [18,19] indicated a link between suppression of complete fusion and *prompt* breakup (prior to reaching the fusion barrier), which reduces the flux of projectile nuclei available to participate in fusion. A more systematic study [20] observed correlation between projectile breakup threshold energies and the ratio of incomplete fusion (a reaction channel that competes with complete fusion). However, to pinpoint which breakup channel directly affect complete fusion, one needs the timescales of each process. In this work, we'll show that with our position sensitive, large solid angle detector array, we were able to obtain the first complete picture of the breakup mechanism of ^{6,7}Li and their reaction timescales.

[a] e-mail: huy.luong@anu.edu.au

2 Experiment

Beams of ^{6,7}Li at energy E_{beam} = 29.0 MeV (bellow the barrier to avoid breakup fragment absorption) were provided by the Australian National University's 14UD tandem electrostatic accelerator. They bombarded a 98.7% enriched ^{208}PbS target, 170 μg cm^{-2} in thickness, supported by a 15 μg cm^{-2} carbon backing. Breakup fragments were detected at back-angle, using a detector system consisted of large area double-sided silicon strip detectors (DSSDs), 400 μm in thickness, in a lamp-shade configuration with apex angle 45°, illustrated in Fig 1. The detectors array has solid angle of 0.6π sr and covered scattering angles θ from 117° to 167°, and 210° in azimuthal angle ϕ.

For breakup of ^{6,7}Li, the most energetically favoured breakup modes involve the production of only two charged fragments, $\alpha + d$ and $\alpha + t$ respectively [21]. Identification of isotopes of hydrogen is thus essential, and made possible through the central ΔE-E detector telescope element (Fig. 1(c)). The identify of other unidentifiable charged particles are deduced through kinematic reconstructions of the breakup event.

3 Mechanism of breakup

The reaction Q-value is determined from the beam energy, energies of the breakup fragments and the recoiling target-like nucleus. This gives information about the state of the target-like nucleus at breakup, but not the state of the projectile-like nucleus as this energy is recovered in the kinetic energy of the breakup fragments. The reconstructed Q spectra for ^{6,7}Li reactions on ^{208}Pb at E_{beam} = 29.0 MeV are shown in Fig. 2. Almost all the yield contribute to sharp

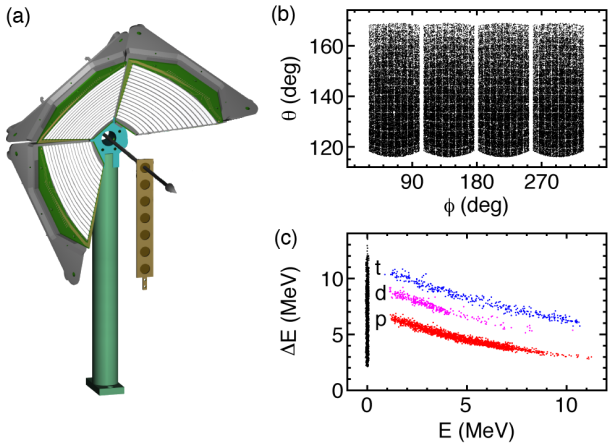

Fig. 1. (a) Arrangement of the basic detector array of four DSSDs, with the beam (arrow) and target ladder. The central detector element contains two DSSDs back to back. (b) The array covers 50° in scattering angle θ and 210° in azimuthal angle ϕ. Pixel separation in each detector is exaggerated for clarity. (c) Typical energy loss ΔE v.s. residual energy E_{res} recorded by the detector telescope, for protons (red), deuterons (magenta), and tritons (blue). Particles (black) that deposit all their energy in the first (ΔE) detector cannot be identified individually, but are identified through the kinematic reconstruction of the breakup event.

peaks in Q, meaning the breakup is indeed almost exclusively binary, with identified breakup modes of $\alpha+\alpha$, $\alpha+t$, $\alpha+d$, and $\alpha+p$. The experimentally obtained Q-values are consistent with the *expected* Q-values, indicated for each breakup mode by vertical bars from the axis.

For ^{6}Li (Fig. 2(a)), the most intense peak, at all bombarding energies, corresponds to breakup of excited states of the projectile into its cluster constituents (α + d), as might be expected. However, breakup into $\alpha+p$ contributed to five distinct peaks in the spectrum, matching the expected Q-values for neutron stripping from the projectile and forming the unbound ^{5}Li, and the five identifiable energy states that ^{209}Pb could populate. The small $\alpha+\alpha$ yield results from pick-up of a neutron and a proton, forming ^{8}Be which subsequently decays into two α-particles.

For ^{7}Li (Fig. 2(b)), breakup into α + t is prominent, as expected. However, production of ^{8}Be (through pick-up of a proton), with subsequent breakup into two α-particles, is much more likely. The Q spectrum shows that the heavy product ^{207}Tl is populated mainly in its four lowest energy states. The $\alpha+d$ breakup mode is triggered by stripping of neutron from the projectile, forming ^{6}Li.

Identification of the reaction processes leading to breakup is not sufficient to understand the interplay between breakup and suppression of complete fusion [16]. Important information on excited states and timescales of the projectile-like nuclei can be recovered in the kinetic energy of the breakup fragments as discussed next.

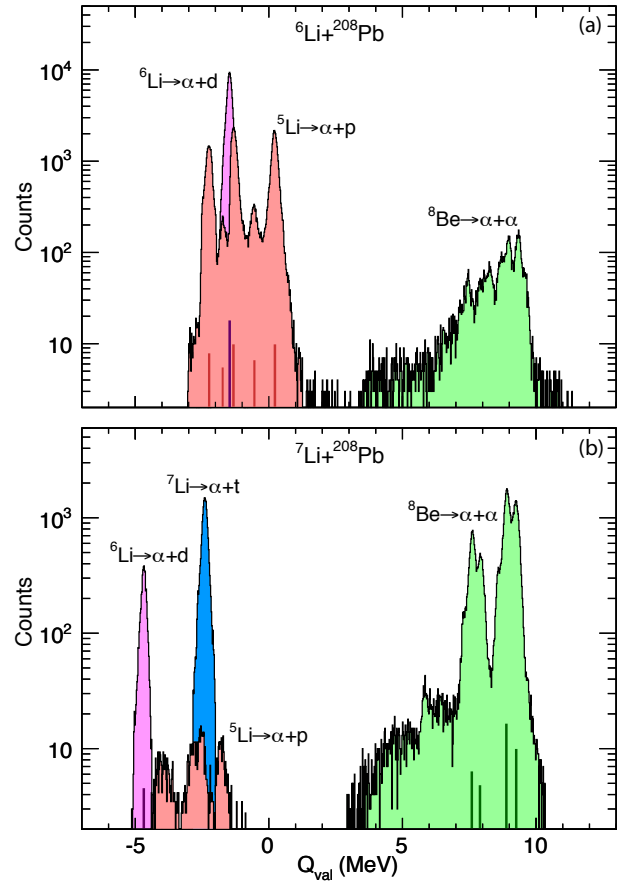

Fig. 2. Measured Q-spectra for the indicated reactions at E_{beam} = 29.0 MeV. Identified breakup modes, consistent with the calculated Q-values (vertical bars), are indicated for $\alpha + p$ (red), $\alpha + d$ (magenta), $\alpha + t$ (blue), and $\alpha + \alpha$ (green) pairs. Patterned area indicate noise consisting of random coincidence and/or event with incomplete energy depositions. (a) The vertical red bars indicate the Q-values for breakup following the population of five identifiable energy states in ^{209}Pb, the green bars the four lowest energy states in ^{206}Tl, and the magenta bar the ^{208}Pb ground-state. (b) The magenta bars indicate the ^{209}Pb ground-state,the blue bar corresponds to the ground state of ^{208}Pb, and the green bars indicate the four lowest energy states of ^{207}Tl.

4 Timescale of breakup

Considering these nuclear collisions classically. The Coulomb field associated with the target nucleus can be seen as a spherical mirror. Breakup of the projectile into two charged fragments after passing the point of closest approach (i.e. after reflection) will give very different fragment trajectories compared to breakup before, as sketched in the two insets of Fig. 3(a) respectively. These different outcomes can be best characterised by the relative energy between the fragments, determined from their relative velocity, and expressed in terms of the measured energies E_i and deduced masses m_i, and the measured angular separation θ_{12} of the fragments

$$E_{rel} = \frac{m_2E_1 + m_1E_2 - 2\sqrt{m_1E_1m_2E_2}\cos\theta_{12}}{m_1 + m_2}. \quad (1)$$

The quantitative dependence of E_{rel} on the internuclear separation at breakup can be determined classically, using a three-body three dimensional model [22,23] developed to relate breakup and fusion.

4.1 Dependency of E_{rel} on breakup trajectories

As an example, E_{rel} distributions have been calculated for breakup of ^{8}Be, from a nominal 1 MeV excitation energy, in the Coulomb field of ^{208}Pb at 29.0 MeV of energy. Fig. 3(a) shows the dependence of E_{rel} on the nuclear separation R_{BU} (or time T_{BU}) at which breakup occurs, relative to the point of closest approach without breakup R_0 (T_0). R_{BU} were uniformly sampled up to 70 fm, and the range of impact parameters considered corresponding to angular momenta up to 79$\hbar$.

The strong variation of the calculated E_{rel} around R_0 (T_0) indicates that breakup close to R_0, and before reflection, will be characterised by a broad E_{rel} distribution (the energy-time uncertainty relation will further broaden E_{rel}). On the other hand, the asymptote towards 1 MeV after R_0 shows that breakup when moving away from the target will be characterised by a peak at lower E_{rel}. Thus the measured E_{rel} spectra are expected to show two components. The first consists of peaks at low E_{rel} values, centred at $E_{rel} = E^* + Q_{BU}$, where E^* is the excitation energy of the state from which breakup occurs and Q_{BU} is the breakup Q-value. These peaks are associated with breakup on the outgoing trajectory, and thus cannot suppress fusion. The second component consists of events extending to high E_{rel}, which are associated with breakup close to the target nucleus. It is these breakup events that must be responsible for the suppression of fusion observed at above-barrier energies [15–17].

4.2 Breakup that competes with fusion

The experimental E_{rel} for each pair of coincident breakup fragments was determined using Eq. 1, shown in Fig. 3(b, c). These spectra, together with the Q-spectra (Fig. 2), give a *complete* picture of breakup in the reactions of these nuclei. For each breakup mode - identified by its Q-value - determination of E_{rel} allows separation between prompt and delayed breakup, i.e. separating breakup components that would ultimately suppress fusion. The experimental E_{rel} distributions (Fig. 3(b,c)) follow qualitatively the expectations from the classical model (Fig. 3(a)), namely narrow peaks at low E_{rel} and broad components extending to high E_{rel}. These E_{rel} spectra have been corrected for detection efficiency for different breakup modes.

Looking at the peaks at low E_{rel} for both the ^{6}Li and ^{7}Li reactions (Fig. 3(b, c)), the E_{rel} spectra for the $\alpha + \alpha$ breakup mode show a sharp peak at 92 keV corresponding to the slow ^{8}Be ground-state decay. This comprises ~half of all the $\alpha + \alpha$ yield. For breakup into $\alpha + d$, the peak at 0.7 MeV corresponds to the decay of the first excited state of ^{6}Li, with a relatively long lifetime of 2.7×10^{-20}s. It is populated by direct excitation of ^{6}Li (Fig. 3(b)) or through n-transfer in the ^{7}Li reaction (Fig. 3(c)).

Considering now breakup with higher E_{rel}, for the ^{6}Li reaction breakup into $\alpha+p$ is very significant. It arises from breakup following neutron transfer and makes the largest contribution to prompt breakup in the reaction with ^{6}Li. The remainder is prompt $\alpha + d$ breakup. For the ^{7}Li reaction, breakup into $\alpha + t$ is prominent, with a wide E_{rel} distribution, indicating essentially all prompt breakup. The largest contribution to prompt breakup for ^{7}Li, however, is from prompt breakup of ^{8}Be, i.e. $\alpha+\alpha$ breakup with higher E_{rel}.

Thus for both the ^{6}Li and ^{7}Li reactions, prompt breakup following transfer is more likely than prompt direct breakup into the projectile cluster constituents. The short time-scale of prompt breakup ($\sim10^{-22}$s), which gives rise to high E_{rel} components, can only be quantitatively interpreted by quantal reaction models [24–26].

5 Conclusion

These measurements have for the first time completely characterised breakup of the weakly bound stable nuclei ^{6,7}Li. Their prompt breakup is found to be triggered by different processes: predominantly *n-stripping* for ^{6}Li, and *p-pickup* for ^{7}Li. The potential implications of this work are far-reaching. Reproducing all the information carried in Fig.2 and Fig.3(b, c) will be a major challenge for the quantum theory of low energy nuclear reactions, requiring new technical developments, and involving questions about the irreversibility or otherwise of coupling to a continuum of relative energy states in breakup. The extreme sensitivity of E_{rel} to the conditions near the point of closest approach of the two nuclei opens the door to investigate dynamical modification of nuclear properties [27] - are the properties of the excited states significantly modified by the close proximity of a heavy nucleus like ^{208}Pb? The demonstration that the reaction dynamics and outcomes can be significantly determined not only by the properties of the two colliding nuclei, but by the ground-state and excited state properties of their neighbours, is a key insight necessary to understand and predict reactions of weakly-bound nuclei at the limits of nuclear existence. Furthermore, the results suggest that in collisions of ^{6,7}Li with all but the lightest nuclei, the dominant nuclear reactions at low energies will lead to their breakup. This needs to be tested experimentally in reactions with nuclei much lighter than ^{208}Pb, and then possible implications for Li abundances in cosmological processes [28,29] investigated. Finally, from these complete data sets, the determination of absolute cross sections for all processes, and their comparison with calculations, promises to solve quantitatively the puzzling behaviour of ^{6,7}Li in near-barrier nuclear reactions, which has remained a challenge for over fifty years.

References

1. R. Ollerhead *et al.*, Phys. Rev. **134**, B74 (1963).

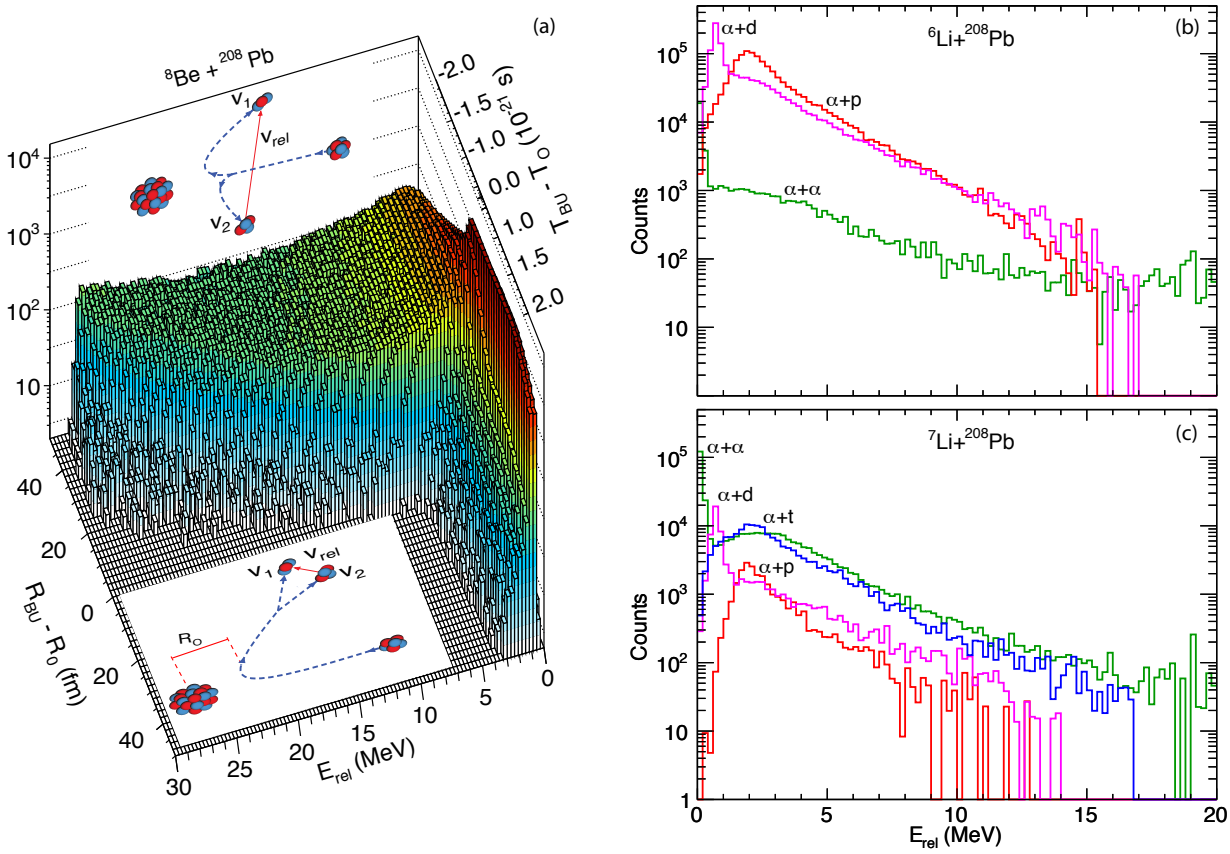

Fig. 3. Simulated E_{rel}-spectra for breakup of ^{8}Be and experimentally measured E_{rel}-spectra for breakup of ^{6,7}Li into $\alpha + p$ (red), $\alpha + d$ (magenta), $\alpha + t$ (blue), and $\alpha + \alpha$ (green) while in collisions with ^{208}Pb at E_{beam} = 29.0 MeV. (a) Graph show the classically calculated dependence of E_{rel} on the nuclear separation (left axis) or time (right axis) at which breakup occurs, relative to the point of closest approach, for 29.0 MeV ^{8}Be + ^{208}Pb. R_{BU} were uniformly sampled up to 70 fm, and impact parameters corresponding to angular momenta up to 79$\hbar$ were included. Breakup prior to reflection, (T_{BU} - T_0) < 0, results in higher E_{rel} values than breakup after reflection (T_{BU} - T_0) > 0. Trajectories of early and late breakup are sketched. (b) The peak at 0.7 MeV for $\alpha + d$ pairs corresponds to decay of the first excited state in ^{6}Li. It is too slow to influence fusion. Thus the dominant breakup mode affecting fusion of ^{6}Li is breakup of ^{5}Li into $\alpha + p$. (c) The low energy peak at 92 keV, from $\alpha + \alpha$ pairs, results from the ground state decay of ^{8}Be. The yield at high E_{rel} for the $\alpha + \alpha$ breakup shows that breakup from excited ^{8}Be is dominant in reactions of ^{7}Li.

2. E. Speth *et al.*, Phys. Rev. Lett. **24**, 1493 (1970).
3. D. L. Disdier *et al.*, Phys. Rev. Lett. **27**, 1391 (1971).
4. R. Ost *et al.*, Phys. Rev. C **5**, 5 (1972).
5. O. Hausser *et al.*, Phys. Lett. B **38**, 75 (1972).
6. K. O. Pfeiffer *et al.*, Nuc. Phys. A **206**, 545 (1973).
7. J. L. Québert *et al.*, Phys. Rev. Lett. **32**, 1136 (1974).
8. A. C. Shotter *et al.*, Phys. Rev. Lett. **53** (1984), 1539.
9. I. J. Thompson *et al.*, Phys. Lett. **106B**, 163 (1981).
10. D. Scholz *et al.*, Nuc. Phys. A **288**, 351 (1977).
11. J. Z. Hesselbarth *et al.*, Phys. A **331**, 365 (1988).
12. R. Ost *et al.*, Z. Phys. **266**, 369 (1974).
13. A. Shrivastava *et al.*, Phys. Lett. B **633**, 463 (2006).
14. D. H. Luong *et al.*, Phys. Lett. B **695**, 105 (2011).
15. M. Dasgupta *et al.*, Phys. Rev. C **70**, 024606 (2002).
16. M. Dasgupta *et al.*, Phys. Rev. C **66**, 041602 (2004).
17. Y. W. Wu *et al.*, Phys. Rev. C **68**, 044605 (2003).
18. D. J. Hinde *et al.*, Phys. Rev. Lett. **89**, 272701 (2002).
19. R. Rafiei *et al.*, Phys. Rev. C **81**, 024601 (2010).
20. L. R. Gasques *et al.*, Phys. Rev. C **79**, 034605 (2009).
21. G. R. Kelly *et al.*, Phys. Rev. C **63**, 024601 (2000).
22. A. Diaz-Torres *et al.*, Phys. Rev. Lett. **98**, 152701 (2000).
23. A. Diaz-Torres, Comp. Phys. Comm. **182**, 1100 (2011).
24. N. Keeley *et al.*, Prog. Part. Nucl. Phys.**59**, 579 (2007).
25. Y. Sakuragi *et al.*, Prog. Theor. Phys. Suppl. **89**, 136 (1982).
26. I. J. Thompson, Comput. Phys. Rep. **7**, 167 (1988).
27. A. B. McIntosh *et al.*, Phys. Rev. Lett. **99**, 132701 (2007).
28. M. Spite *et al.*, Nature **297**, 483 (1982).
29. H. Utsunomiya *et al.*, Phys. Lett. B **416**, 43 (1988).